Passive RFID System for Object Shape Estimation

G. Alvarez-Narciandi, J. Laviada, M. R. Pino, F. Las-Heras
Área de Teoría de la Señal y Comunicaciones, Universidad de Oviedo
Edif. Polivalente, Mod. 8, Campus Universitario de Viesques. E-33203, Gijón (Asturias), Spain
Email: {ganarciandi,jlaviada,mpino,flasheras}@tsc.uniovi.es

***Abstract*—In this paper the feasibility of using low-cost Radio Frequency IDentification (RFID) technology to estimate the shape of objects is tested. Two reconstruction techniques are compared: Computed Tomography (CT) and Radio Tomographic Imaging (RTI). For this purpose, a setup comprising a linear array of RFID tags and a transmitting antenna is proposed. Several simulations were carried out using two different models (a rectangular prism and two cylinders) and the performance of both techniques was tested for different values of angular sampling. Finally, the reconstructed images are presented and the performance of CT and RTI is discussed.**

***Index Terms*—Radio Frequency IDentification (RFID), Radio Tomographic Imaging (RTI), Computed Tomography (CT), Received Signal Strength (RSS).**

I. Introduction

The aim of this paper is to test the performance of two different techniques to estimate the shape of objects employing RFID technology: Computed Tomography (CT) and Radio Tomographic Imaging (RTI). There are several techniques that have been successfully applied to reconstruct the shape of objects using EM signals. Among these techniques, CT, which is widely used in medical systems [1], consists of reconstructing the cross-section of an object given its projections. These projections are acquired by transmitting signals across the object and receiving it at a set of sensors. On the other hand, RTI is a technique, proposed in [2], [3], [4], that has been used for localization purposes. In particular, it has been used in device-free user localization employing low-cost sensor networks with both active [2], [3] and passive nodes [5]. In a similar way to CT, it is based on the attenuation or shadowing that a radio signal suffers when it passes through an object. RTI systems are based on a wireless sensor network deployed in the area of interest.

In this context, we propose to test these techniques (CT and RTI) using an array of UHF RFID passive tags and a transmitting antenna. Due to the low bandwidth and relative low frequency of this technology (the European UHF RFID band spans from 865.6 MHz to 867.6 MHz), the expected resolution of the system is not high. However, the system is expected to estimate the shape of medium size objects with low computational complexity (in contrast to other imaging techniques such as those based on global optimization, which can be more accurate at the expense of a high computational cost [6], [7]). In the next sections, the proposed system setup is described and simulation results for both techniques are discussed.

II. System description

The scheme of the proposed setup is depicted in Fig. 1. As can be seen, there is an array of N_{tags} uniformly spaced RFID tags separated a distance d facing the transmitting antenna. The object under test (OUT) is placed between them. In order to obtain enough information to estimate the shape of the OUT (in this case, its 2D contour), it is necessary to take measurements for several incident angles, N_{inc}. To achieve this, the OUT can be rotated or, equivalently, the array of tags and the antenna can be rotated around it.

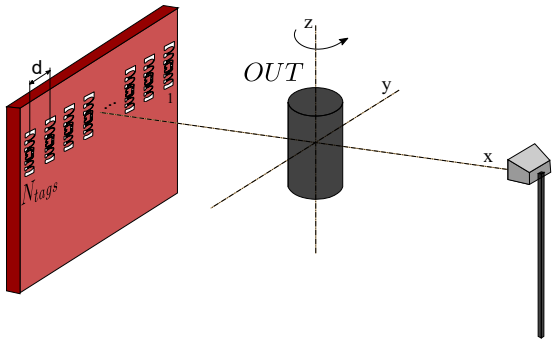

Fig. 1. Scheme of the proposed setup.

In the context of CT, the proposed setup has a fan-beam imaging geometry and the array of tags is a flat detector. With this type of geometry and detector, one of the possible approaches to reconstruct the image of the object consists of converting the fan-beam rays to parallel-beam rays and then computing the filtered-backprojection of the data [1]. Each projection is the line integral for a given view (angle of incidence, θ) and a position (given by the coordinates of the sensors, s) as illustrated in Fig. 2. It must be pointed out that, employing a flat detector, the projections are uniformly-spaced sampled (in this case, separated a distance d), but the angular spacing between them is not uniform. In this case, the projection for a given incidence angle is given by the Received Signal Strength (RSS) measurements of the signal backscattered by each RFID tag.

Regarding the RTI technique, the system is based on the work presented in [2] and [5]. Therefore, the area of interest (between the array of tags and the antennas) is discretized in a rectangular grid of N_{pixels} pixels. The attenuation model is given by

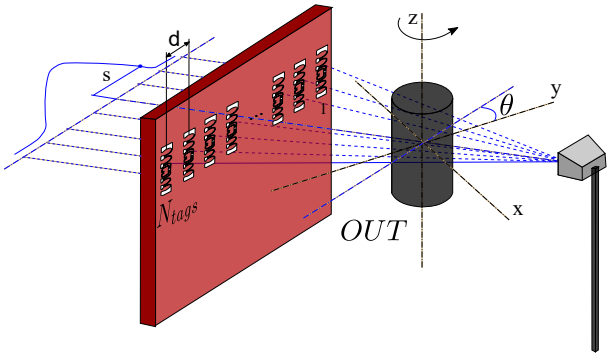

Fig. 2. Scheme of the proposed setup with the main parameters to define each projection when using CT.

$$\Delta y = W\Delta x + n, \tag{1}$$

where the attenuation of each link, Δy, is regarded as a linear combination of the attenuation of each pixel, i.e., the unknown image, Δx. The matrix W is a weighting matrix for every pixel, tag and antenna combination and n is the noise.

It must be pointed out that, using this scheme, each link accounts for the propagation of the signal from the transmitting antenna to an RFID tag and the round-trip of the backscattered signal. The weighting matrix has dimensions $N_{tags}N_{inc} \times N_{pixels}$ and the weight of the pixel j of the link i is given by

$$\omega_{ij} = \frac{1}{d_{tx,tag(i)}} \begin{cases} 1 \text{ if } d_{tx,j} + d_{j,tag(i)} < d_{tx,tag(i)} + \gamma \\ 0 \quad \text{otherwise} \end{cases}, \tag{2}$$

where $d_{tx,j}$ is the distance from the transmitter to the pixel j; $d_{j,tag(i)}$ is the distance from the pixel j to the tag of the link i; $d_{tx,tag(i)}$ is the distance between the transmitter and the tag of the link i; and where it has been taken into account that pixels in the direct path (or near it) from the transmitter-tag pair of the link i have a stronger influence on the attenuation of that link. The amount of pixels considered for each link is controlled by γ. In order to compute the attenuation of each link, a calibration stage is performed prior to the measurements. The calibration consists of recording measurements of the RSS of the signal backscattered by each tag at the transmitter without any objects in the scene. Then, when an object is being measured, the obtained RSS values can be subtracted from those gathered during the calibration. As RTI is an ill-posed problem, the Tikhonov regularization (approximating the derivative operator by a difference matrix) is used as proposed in [2]. Finally, the image is computed as

$$\hat{x} = (\boldsymbol{W}^T\boldsymbol{W} + \alpha(\boldsymbol{D}_X^T\boldsymbol{D}_X + \boldsymbol{D}_Y^T\boldsymbol{D}_Y))^{-1}\boldsymbol{W}^T\Delta_y, \tag{3}$$

where α is the regularization parameter and $\boldsymbol{D}_X$ and $\boldsymbol{D}_Y$ are the difference operators for the horizontal and the vertical directions respectively.

III. Numerical results

Several simulations have been carried out using the EM simulation software *FEKO* [8]. The number of RFID tags of the array was set to $N_{tags} = 60$ tags separated 0.13λ and two different geometries have been simulated for both CT and RTI. In both cases the OUT was separated 2 m from the line of tags.

The first OUT was a rectangular prism of constant cross-section of 0.6×0.8 m. The cross-section was reconstructed using both techniques taking measurements every $10°$ ($\Delta\phi = 10°$) and every $30°$ ($\Delta\phi = 30°$). The obtained results for $\Delta\phi = 10°$ are depicted in Fig. 3(a) and Fig. 3(b) for RTI and CT, respectively. The reconstructed cross-sections for $\Delta\phi = 30°$ are shown in Fig. 3(c) and Fig. 3(d) for RTI and CT, respectively. As can be seen, the estimated cross-section is similar for every configuration: the size of the image is estimated, but there are problems with the corners of the cross-section. However, the reconstructed image is noisier when using RTI than when employing CT and, as expected, the image is noisier when the angular sampling is lower.

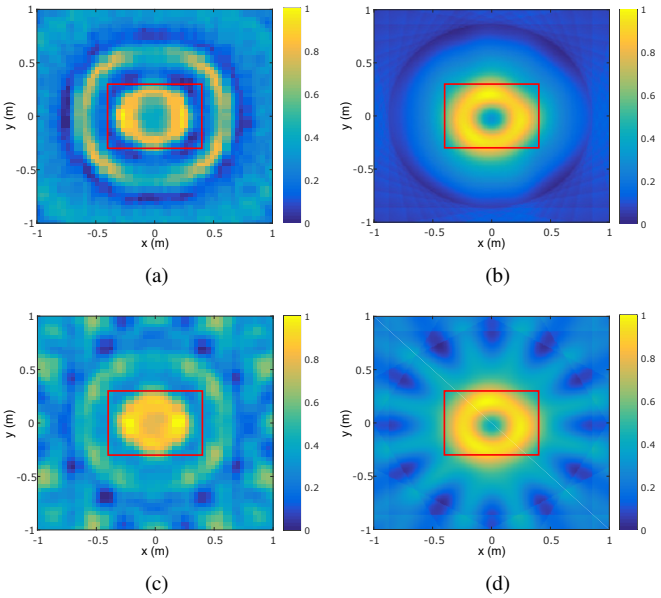

Fig. 3. Reconstructed cross-section of the simulated rectangular prism for $\Delta\phi = 10°$ using RTI a) and CT b) and for $\Delta\phi = 30°$ using RTI c) and CT d).

The second simulated scenario consists of two cylinders of radius $r = 0.2$ m which were separated 0.75 m. As in the first simulated geometry, two different angular sampling values were tested ($\Delta\phi = 10°$ and $\Delta\phi = 30°$). The obtained results for $\Delta\phi = 10°$ are depicted in Fig. 4(a) and Fig. 4(b) for RTI and CT, respectively. The reconstructed cross-sections for $\Delta\phi = 30°$ are shown in Fig. 4(c) and Fig. 4(d) for RTI and CT, respectively. As can be observed, when $\Delta\phi = 30°$ and RTI is used there is a great amount of noise in the image. Hence, although it is possible to infer that there two main peaks in the image, the quality of the results is very poor. In the case of CT, despite the low contrast between the estimated cross-section of

the cylinders and the background, there is a good agreement between the reconstructed cross-section of both cylinders and the separation between them and the simulated model. When $\Delta\phi = 10°$, there are two clear targets using either RTI or CT. However, even though the separation between the two targets matches the distance between both cylinders, the size of the cylinders is only well estimated when employing CT.

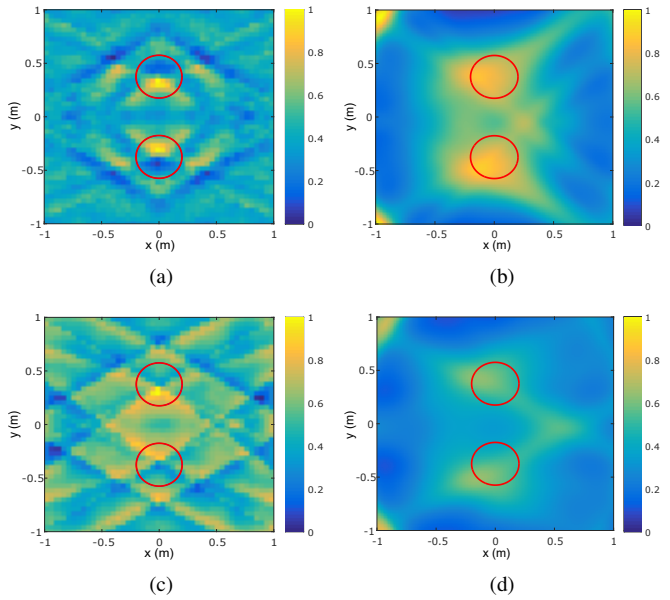

Fig. 4. Reconstructed cross-section of the two simulated cylinders separated 0.75 m for $\Delta\phi = 10°$ using RTI a) and CT b) and for $\Delta\phi = 30°$ using RTI c) and CT d).

IV. Conclusion

In this paper the capacity of reconstructing the shape of objects with a passive RFID based system employing RTI and CT was investigated. For that purpose, numerical simulations of two different scenarios were carried out using an EM simulator. The reconstructed images of the first model, a rectangular prism, showed that the size of the estimated object was similar to the size of the model using both RTI and CT, although the corners of the rectangular cross-section were smoothed. The results obtained for the second model when using an angular sampling of thirty degrees are very noisy, especially employing RTI. However, when the angular sampling was increased to ten degrees, both cylinders were detected with both techniques. The best results were achieved using CT as not only the distance between the cylinders, but also their size was in very good agreement with the simulated models.

Results have shown that the shape of a medium electric size object can be estimated using the proposed setup. The CT appears to be more robust despite the RFID frequency band.

Future research regarding this approach includes the deployment of the proposed setup in a real scenario and compare the performance of the obtained simulation results with measurements. In addition, both monostatic and bistatic setups can be compared. Finally, it must be pointed out that this technique could be easily scaled in frequency in order to improve the resolution of the system.

Acknowledgment

This work has been supported by the Gobierno del Principado de Asturias (PCTI)/FEDER-FSE under project GRUPIN14-114; by the Ministerio de Ciencia e Innovación of Spain/FEDER under projects TEC2014-55290-JIN and MIRIIEM-TEC2014-54005-P and under the FPU grant FPU15/06431.

References

[1] G. L. Zeng, "Advanced sampling techniques in electromagnetics," in *Medical Image Reconstruction. A conceptual Tutorial.* Springer, 2010.

[2] J. Wilson and N. Patwari, "Radio tomographic imaging with wireless networks," *IEEE Trans. Mobile Comput.*, vol. 9, no. 5, pp. 621–632, May 2010.

[3] ——, "See-through walls: Motion tracking using variance-based radio tomography networks," *IEEE Trans. Mobile Comput.*, vol. 10, no. 5, pp. 612–621, May 2011.

[4] J. Wilson, N. Patwari, and F. Vasquez, "Regularization methods for radio tomographic imaging," in *2009 Virginia Tech Symposium on Wireless Personal Communications*, 2009.

[5] B. Wagner, N. Patwari, and D. Timmermann, "Passive rfid tomographic imaging for device-free user localization," in *2012 9th Workshop on Positioning Navigation and Communication (WPNC)*, 2012.

[6] Y. Álvarez, M. García-Fernández, L. Poli, C. García-González, P. Rocca, A. Massa, and F. Las-Heras, "Inverse scattering for monochromatic phaseless measurements," *IEEE Trans. Instrum. Meas.*, vol. 66, no. 1, pp. 45–60, 2017.

[7] C. C. Chiu and P. T. Liu, "Image reconstruction of a perfectly conducting cylinder by the genetic algorithm," *IEE Proc. Microw., Antennas Propag.*, vol. 143, no. 3, pp. 249–253, 1996.

[8] Altair. (2017, 10) FEKO EM simulation software. [Online]. Available: https://www.feko.info/